Appl. Phys. B 47, 361–366 (1988)

Applied Physics B Photophysics and Laser Chemistry

Rapid Communication

X-Ray Production by Irradiation of Solid Targets with Sub-Picosecond Excimer Laser Pulses*

G. Kühnle[1], F. P. Schäfer[1], S. Szatmári[1], and G. D. Tsakiris[2]

[1] Max-Planck-Institut für biophysikalische Chemie, Abteilung Laserphysik, Postfach 2841, D-3400 Göttingen, Fed. Rep. Germany

[2] Max-Planck-Institut für Quantenoptik, Postfach 1513, D-8046 Garching, Fed. Rep. Germany

Received 12 October 1988/Accepted 14 October 1988

Abstract. A table-top excimer laser system generating sub-ps pulses was used to irradiate solid targets at intensities of up to 4×10^{15} W/cm^2. Soft X-ray spectra of various materials were measured. The X-ray conversion efficiencies were between 1–5%. Streak camera measurements showed instrument-limited X-ray pulse duration of a few ps.

PACS: 52.50.Jm

There is presently a strong interest in plasmas produced by picosecond and sub-picosecond laser pulses [1–5]. Beside fundamental aspects of plasma physics at this time scale and highest light intensities there are also new prospects of developing a laboratory X-ray laser using such a plasma as the active medium [6].

We report on some experiments in which we irradiated various solid targets with sub-picosecond excimer laser pulses and observed the spectra and the time behavior of the emitted X-rays.

1. Experimental

We used a hybrid dye-excimer laser system that delivers 10 mJ pulses at 248.5 nm in typically 500 fs. Since the pulse is strongly chirped, it can be compressed to 60 fs [7]. The output was focussed with a quartz plano-convex lens of 140 mm focal length onto a plane target, which was placed in a vacuum chamber. The angle between the target normal and the optical axis changed between 0° for spectra measurements and 11° for X-ray streak camera measurements. The focal spot diameter was determined by spherical aberrations of the focussing lens. The calculated diameter was 30 μm for the beam cross section 10 mm × 22 mm (the diffraction limited spot diameter is 8 times smaller). We measured the spot diameter with a pinhole camera (magnification 10, resolution 20 μm). The radiation was filtered with a 0.8 μm aluminum foil to record only the radiation in the regions 8 Å–40 Å and 170 Å–350 Å on a film (Kodak 101-01). The longer wavelengths radiation is emitted by the already expanded and cooled plasma and measuring these would lead to a much larger spot size. The measured size (FWHM) of the short wavelength radiation source was 37 μm. In order to calculate the intensities incident on the target correctly from the pulse energy, the focal spot diameter and the pulse duration, we had to take into account that the pulse front is bent in the form of a paraboloid by a spatial filter and the focussing lens [8] which lengthens the pulse on the target. The effective pulse duration seen by the target was calculated as 0.9 ps, and the intensities stated have been corrected for this effect. Some of the experiments were performed with an additional amplifier (EMG 401, Lambda Physik) which enhanced the output energy to 70 mJ in a beam of 25 mm × 45 mm cross-section. In this case we used an expanding telescope before the amplifier and a quartz plano-convex lens of 500 mm focal length for focussing on the target. The spot diameter was here

* Partially based on the plenary talk "X-Ray Generation by Sub-Picosecond UV Laser" by F. P. Schäfer, G. Kühnle, S. Szatmári, and M. Steyer, presented at the XVI Int. Quant. Electron. Conf., Tokio, July 18–21, 1988, Technical Digest (The Japan Society of Applied Physics) p. 2

also determined by the spherical aberration of the lens (calculated diameter: 40 μm which is 6 times larger than diffraction limited diameter, measured diameter 50 μm). The pulse duration seen by the target using the amplifier was calculated as 1.5 ps. We have not yet performed experiments with compressed pulses, since the absorption of most optical materials for this high intensity uv light is too high and suitable large prisms made from MgF_2 needed for the compression of the full cross-section beam were not available at the time of these measurements.

The spectra were recorded using a simple transmission spectrograph with a 1000 lines/mm free-standing gold grating in a 100 μm pinhole (Dr. J. Heidenhain GmbH, D-8225 Traunreut, FRG) with a calculated spectral resolution between 5 Å (for 6 Å radiation) and 10 Å (for 211 Å radiation). The angle between the target normal and the optical axis of the spectrograph was 45° and the solid angle seen by the spectrograph was 2.4×10^{-8} sr. The spectra were recorded on an absolutely calibrated film (Kodak 101-01) [9], scanned with a micro-densitometer and evaluated in a personal computer. Since the grating efficiency and the film sensitivity is known, we can calculate the spectral X-ray energy density (J/(Å · sr)). Assuming that the X-ray emission is isotropic in 2π solid angle, one may calculate the total X-ray energy in a certain spectral range by integrating the spectra over this spectral range and multiplying the result with 2π. Comparing the X-ray energy with the incident pulse energy, one gets the conversion efficiency, which was approximately 0.5% (lower Z materials) −2% (higher Z-materials) for the lower energy pulses (1.6×10^{15} W/cm^2, 1.4×10^3 J/cm^2) and 2% (lower Z materials) −5% (higher Z materials) for the higher energy pulses (3.7×10^{15} W/cm^2, 5.6×10^3 J/cm^2) in the spectral range 50 to 250 Å with a statistical accuracy of a factor of 2. Further work is in progress to determine exactly what fraction of the incident energy is absorbed at the intensities used here so that the intrinsic conversion efficiency can be calculated.

The time behavior of the X-ray emission was studied with an X-ray streak camera developed by one of us (G.D.T.) [10]. For time calibration of the streak camera, we placed a 60 mm long quartz block in one half of the beam to provide two pulses with a delay of 129.4 ps between them on the target. Recording the two X-ray pulses emitted from the plasma on film we calculated the deflection speed on the streak camera screen to be 98–105 ps/mm. Taking into account the total magnification of 1.13 and the imaging resolution of 100 μm in the slit plane of the camera we obtained a minimal resolution of 11–12 ps. In our experiment we used a slit of 300 μm width which means that our time resolution was geometrically limited to 35–38 ps.

Spectrally and temporally integrated relative conversion efficiencies were measured using a windowless high voltage vacuum biplanar photodiode at 50 Ω and a Tektronix 7104 oscilloscope. Since the bandwidth of the oscilloscope is 1 GHz, the maximum of the oscilloscope trace is proportional to the time-integral over approximately 200 ps of the X-ray pulse.

In all measurements the target was shifted between shots (5 to 50 μm per shot, depending on the total number of shots), so that each part of the sample was irradiated by 1 to 10 shots on the average.

2. Results

Figure 1 shows an aluminum spectrum normalized to the incident pulse energy recorded with the sub-ps pulse at 1.6×10^{15} W/cm^2 (1.4×10^3 J/cm^2) (dotted line) and for comparison the same spectrum taken with a 15 ns pulse at 1.6×10^{12} W/cm^2 (2.4×10^3 J/cm^2) (solid line, this spectrum is 3 times down-scaled). All lines can be clearly assigned to Al^{3+} through Al^{8+} (transitions from an excited level of the outer electron to $1s^2 2s^2 2p^x$). The larger width of the lines in the ns-spectrum can be attributed to the expansion of the plasma during the 15 ns long irradiation time, which leads to a decreased spatial and hence spectral resolution in our spectrograph. The different relative heights of the lines in the two spectra are a result of the different plasma temperatures, whereas the difference in the absolute heights (roughly a factor of 3) of the lines is due to the different conversion efficiencies. The reason for the larger conversion efficiency of the 15 ns pulse may be the fact that the later part of the pulse is

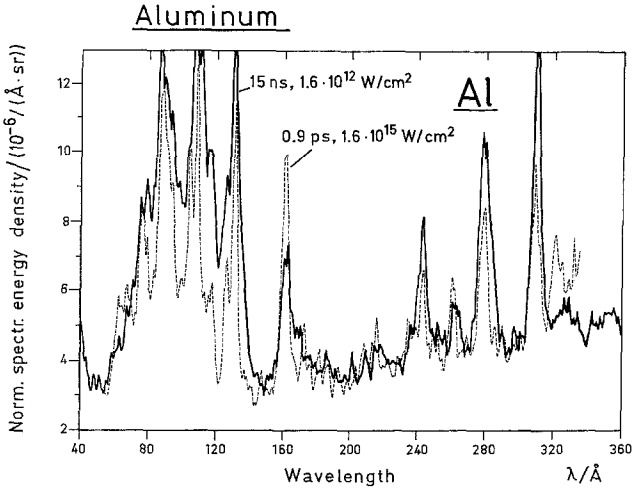

Fig. 1. Aluminum spectra normalized to the incident pulse energy with the sub-ps pulse at 1.6×10^{15} W/cm^2 (dotted line) and with a 15 ns pulse at 1.6×10^{12} W/cm^2 (solid line, this spectrum is 3 times down-scaled) measured with a transmission spectrograph (resolution 5–10 Å)

coupled more strongly into the plasma that was created by the earlier part of the pulse while for some application, where maximum efficiency is mandatory, the 15 ns pulses would be used, other applications, as e.g. new X-ray laser schemes [1, 6], that need the shortest possible pulses, have to take into account that these pulses yield the reported lower efficiencies.

Figure 2 shows two aluminum spectra taken at different intensities, namely 2.6×10^{14} W/cm^2 (3.9×10^2 J/cm^2) and 3.7×10^{15} W/cm^2 (5.6×10^3 J/cm^2). The increase of the continuum and the shift of its maximum to shorter wavelengths with increasing intensity is quite obvious, which is a result of the much higher temperature achieved in the plasma with the higher intensity pumping. In contrast to usual practice, the intensities were not varied by changing the spot diameter but rather by attenuating the beam using a dielectric coated mirror (quartz substrate with two well polished parallel surfaces) in transmission at different incident angles where the narrow-band coating had 100% reflectivity for 0° incident angle. Using this technique one could continuously change the transmission from 0% to 60% having only a very small (negligible compared to the beam size) parallel beam shift. As we will show later, varying the energy and not the spot size leads to more consistent results.

Figure 3 shows a spectrum of carbon, obtained by irradiation of a carbon rod at 3.7×10^{15} W/cm^2 (5.6×10^3 J/cm^2). Three groups of the K-shell transitions of C^{5+} and C^{4+} show up very clearly, namely $3p^1 - 1s^1$

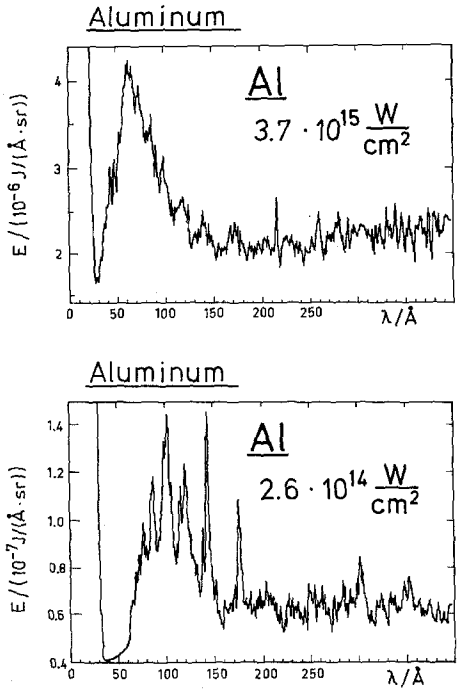

Fig. 2. Aluminum spectra at 2.6×10^{14} W/cm^2 and 3.7×10^{15} W/cm^2 (intensity is varied by varying the pulse energy) measured with a transmission spectrograph (resolution 5–10 Å)

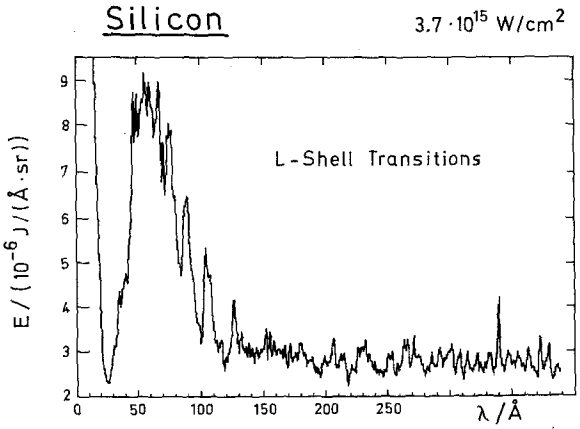

Fig. 4. Silicon spectrum at 3.7×10^{15} W/cm^2 with L-shell transitions measured with a transmission spectrograph (resolution 5–10 Å)

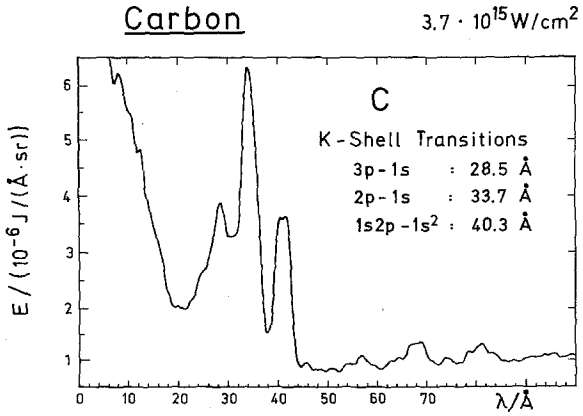

Fig. 3. Carbon spectrum at 3.7×10^{15} W/cm^2 with K-shell transitions measured with a transmission spectrograph (resolution 5–10 Å)

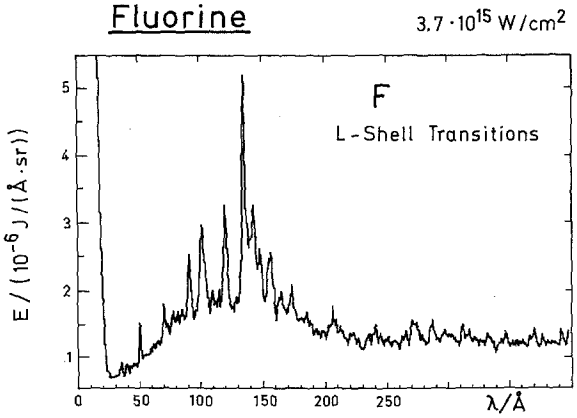

Fig. 5. Fluorine spectrum at 3.7×10^{15} W/cm^2 with L-shell transitions measured with a transmission spectrograph (resolution 5–10 Å)

at 28.5 Å, $2p^1-1s^1$ at 33.7 Å, and $1s^12p^1-1s^2$ at 40.3 Å.

Figures 4–6 show spectra of silicon, fluorine and gold, all taken at the same intensities as for Fig. 3. Most of the lines in the silicon and fluorine spectra are, like in the aluminum spectrum, transitions of the *L*-shell, whereas the gold spectrum shows O-shell transitions. One can estimate the energy per ion of the ionization state, which shows the strongest lines in the measured spectrum, by adding all ionization energies of the outer electrons of all lower ionized states. In our case we obtained 500–1500 eV/ion.

For the streak-camera measurements different filters were used to separate the spectral regions, namely 0.1 μm thick carbon for wavelengths <300 Å, and 2.3 μm thick aluminum for the regions from 8 Å–30 Å and 170 Å–250 Å. Figure 7 shows the pulse shape for a

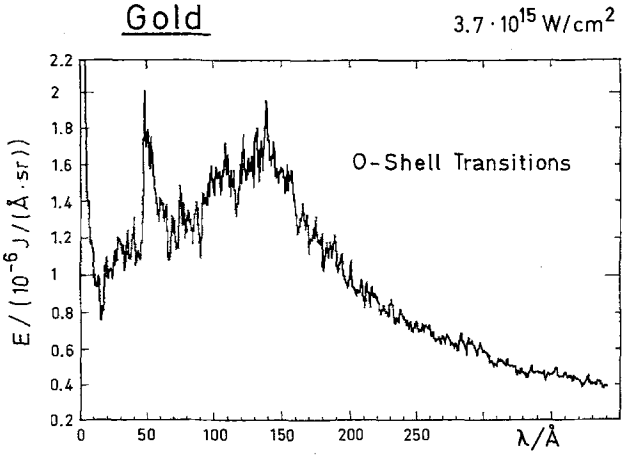

Fig. 6. Gold spectrum at 3.7×10^{15} W/cm^2 with O-shell transitions measured with a transmission spectrograph (resolution 5–10 Å)

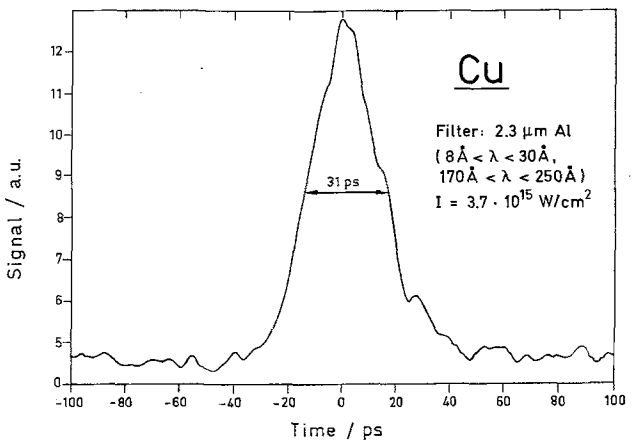

Fig. 7. Pulse shape for a copper target at wavelengths 8 Å–30 Å and 170 Å–250 Å measured with a 2.3 μm thick aluminum foil filtered X-ray streak camera (calculated resolution 35–38 ps)

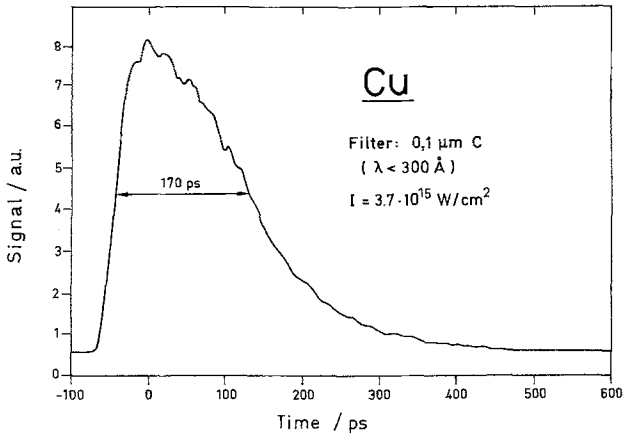

Fig. 8. Pulse shape for a copper target at wavelengths <300 Å measured with a 0.1 μm thick carbon foil filtered X-ray streak camera (calculated resolution 35–38 ps)

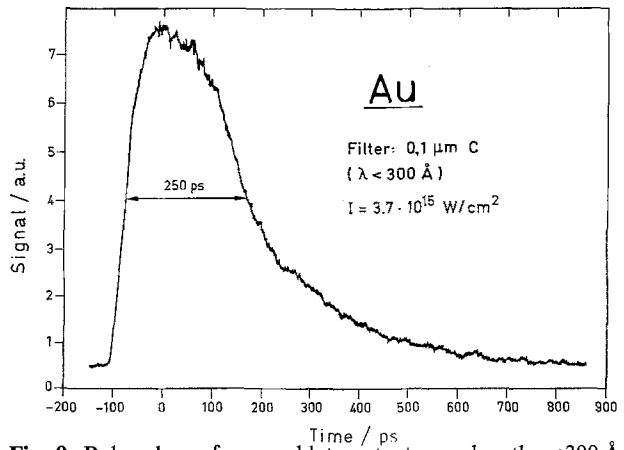

Fig. 9. Pulse shape for a gold target at wavelength <300 Å measured with a 0.1 μm thick carbon foil filtered X-ray streak camera (calculated resolution 35–38 ps)

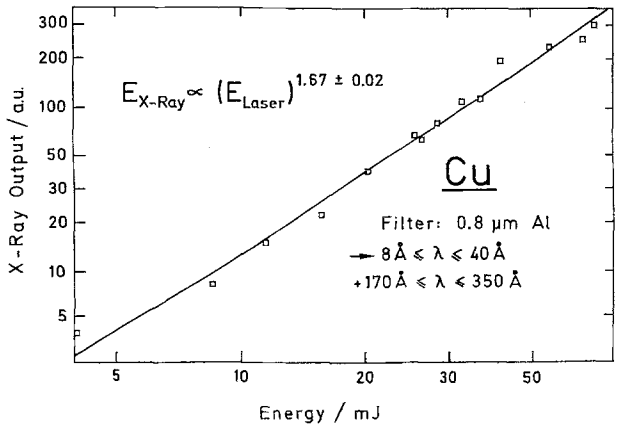

Fig. 10. Energy dependence of X-ray production in the range 8 Å–40 Å and 170 Å–350 Å (only the pulse energy was changed) measured with an 0.8 μm thick aluminum foil filtered windowless biplanar vacuum photodiode

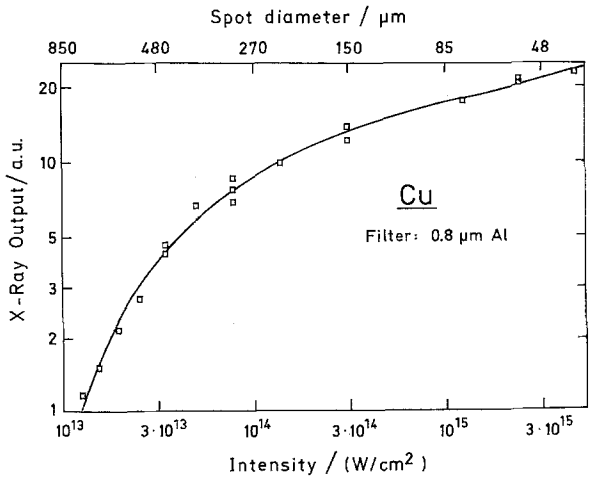

Fig. 11. Intensity dependence of X-ray production in the range 8 Å–40 Å and 170 Å–350 Å (only the laser spot size was changed) measured with an 0.8 µm thick aluminum foil filtered windowless biplanar vacuum photodiode

copper target at short wavelengths, which is clearly instrument-limited, while Fig. 8 shows the pulse including the long wavelength region, which is evidently dominated by the slow recombination radiation. This can be seen even more clearly in Fig. 9, which shows the pulse shape for a gold target in the long wavelength region.

The energy dependence of the time integrated X-ray output, when the beam was attenuated with the dielectric mirror, is shown in Fig. 10 for a copper target filtered with 0.8 µm thick aluminum. The slope of the straight line of this power plot is 1.67 ± 0.02. There is no indication of incipient saturation even at a laser energy of 80 mJ.

A totally different behavior is shown, when the intensity dependence of the X-ray output is determined by changing only the distance between the focussing lens and the target in order to change the spot diameter, while the energy was kept constant at 70 mJ. Here the slope of the curved line is between 0.2 and 2.0. It decreases significantly with increasing intensity. A possible reason for this behavior is the change of the cooling conditions by changing the ratio of surface to volume of the irradiated sample. This demonstrates the importance of measuring the intensity dependence by changing the pulse energy, while all other parameters are kept constant.

3. Discussion

The spectra reported here show clearly that a highly ionized plasma is created when irradiating solids with picosecond and sub-picosecond pulses of ultraviolet light at intensities of up to 3.7×10^{15} W/cm^2 (5.6×10^3 J/cm^2). A question that arises in this context is whether the part of the approximately 15 ns long ASE pulse (the short pulse is centered near the maximum of the ASE pulse), which reaches the target before the short pulse, is responsible for this plasma formation, which would then be heated by the sub-ps pulse. The ≈ 5 ns long ASE prepulse of our laser system (including the EMG 401) is less than 10% of the energy of the short pulse and only 30% of the prepulse has the same divergence angle as the short pulse (the rest of the prepulse has a 100 times larger divergence angle than the short pulse and is therefore negligible). This results then in a peak power that is more than five orders of magnitude lower than that of the sub-ps pulse, giving an intensity of 3×10^{10} W/cm^2. We could not detect any radiation in the soft X-ray range at this low intensity. This means that there was no hot plasma produced, but does not exclude a cold plasma. To check this we investigated the incident angle dependence of the short-pulse X-ray emission for *p*-polarized light. The measurement showed no significant dependence of the X-ray emission on the angle of the incidence. If a cold plasma had been produced by the low intensity prepulse, resonance absorption in the cold plasma would have produced a strong incident angle dependence of the X-ray emission [2]. Therefore we must conclude that it is really the sub-ps pulse that creates the plasma.

Simulation of the early stage of plasma formation using a modified collisional-radiative model [11] makes it plausible that the hard components of the X-ray radiation are already emitted from the plasma developed during the laser pulse irradiation, whereas the long wavelength recombination radiation will create a long tail. Unfortunately, present X-ray streak cameras are too slow to verify this picture. Nevertheless the scan shown in Fig. 7 at least demonstrates a pulse duration of at most a few ps, since the observed pulse width of 31 ps does not show any increase beyond the instrument limit.

This work will be extended to higher intensities using compressed pulses and time-corrected focussing optics. We also intend using higher spectral resolution with a grazing incidence spectrograph to determine plasma temperatures.

4. Conclusion

Using a table-top excimer laser system, which generates sub-ps pulses, we investigated the spectral and temporal behavior of the X-rays emitted from the produced plasma for various target materials.

We also measured conversion efficiencies and showed the importance of well defined experimental

conditions measuring the intensity dependence of the conversion efficiencies.

Acknowledgements. Discussions with Dr. R. Sigel and Dr. K. Eidmann, Garching, and Dr. M. Steyer, Göttingen, are gratefully acknowledged. This work has been supported by the Bundesministerium für Forschung und Technologie and by the Deutsche Forschungsgemeinschaft.

References

1. R.W. Falcone, M.M. Murname: In *Short Wavelength Coherent Radiation: Generation and Applications*, ed. by D.T. Attwood, J. Bokor (AIP, New York 1986) p. 81
2. D.G. Stearns, O.L. Landen, E.M. Campbell, J.H. Scofield: Phys. Rev. A **37**, 1684 (1988)
3. P.R. Wood, W.T. Silfvast, H.W.K. Tom, W.H. Knox, R.L. Fork, C.H. Brito-Cruz, M.C. Downer, P.J. Maloney: Appl. Phys. Lett. **53**, 654 (1988)
4. O.L. Landen, E.M. Campbell, M.D. Perry: Opt. Commun. **63**, 253 (1987)
5. D. Kühlke, U. Herpers, D. von der Linde: Appl. Phys. Lett. **50**, 1785 (1987)
6. F.P. Schäfer: J. Phys., Coll. C6, Suppl. 10, **47**, C6-149/C6-150 (1986)
7. S. Szatmári, F.P. Schäfer: Opt. Commun. **68**, 196 (1988)
8. S. Szatmári, G. Kühnle: Opt. Commun. (in press)
9. T. Kishimoto: Report of Max-Planck-Institut für Quantenoptik, Garching, 108 (1985) 70
10. G.D. Tsakiris: 18th Int'l. Congress on High Speed Photography and Photonics, Aug. 26–Sept. 2 (1988), Xi'an, Sheanx, China, SPIE Proceedings Vol. 1032 (in press)
11. M. Steyer: Dissertation, Göttingen, 1988

Responsible for Advertisements: E. Lückermann, G. Probst, Heidelberger Platz 3, D-1000 Berlin 33, Tel. (030) 8207-0, Telex 01-85411, FAX (0) 30/8214091
Responsible for the Text: H. K. V. Lotsch, Tiergartenstrasse 17, D-6900 Heidelberg, Tel. (0) 6221/487253, Telex 461723, FAX (0) 6221/43982
Printers: Brühlsche Universitätsdruckerei, Giessen

Springer-Verlag GmbH & Co. KG, D-1000 Berlin 33